Molecular Cancer Research

ROS1 and ALK Fusions in Colorectal Cancer, with Evidence of Intra-tumoral Heterogeneity for Molecular Drivers

Dara L. Aisner, Teresa T. Nguyen, Diego D. Paskulin, et al.

Mol Cancer Res Published OnlineFirst December 2, 2013.

ROS1 and *ALK* Fusions in Colorectal Cancer, with Evidence of Intra-tumoral Heterogeneity for Molecular Drivers

Dara L. Aisner[1*], Teresa T. Nguyen[1*], Diego D. Paskulin[1,2], Anh T. Le[1], Jerry Haney[1], Nathan Schulte[1], Fiona Chionh[3], Jenny Hardingham[4], John Mariadason[3], Niall Tebbutt[3], Robert C. Doebele[1], Andrew J. Weickhardt[1,3,#]and Marileila Varella-Garcia[1,#]

[1]University of Colorado Cancer Center, Aurora, Colorado, USA

[2]Federal University of Rio Grande do Sul, Department of Genetics, Porto Alegre, Brazil

[3]Ludwig Institute for Cancer Research, Melbourne, Australia

[4]The Basil Hetzel Institute, The Queen Elizabeth Hospital, Adelaide, Australia

*DLA and TTN contributed equally to this manuscript.

[#] AJW and MVG share senior position authorship

CONFLICT OF INTEREST

Dara L. Aisner had educational speaker engagement with Abbott Molecular and Marileila Varella-Garcia received research grant and had educational speaker engagement with Abbott Molecular. No other authors have conflicts of interest to declare.

Corresponding Author:

Marileila Varella Garcia, PhD

University of Colorado School of Medicine Anschutz Medical Campus

12801 E 17th Ave, L18-8118

Mail stop 8117

Aurora, CO 80045, USA

Marileila.Garcia@ucdenver.edu

Abstract

Activated *ALK* and *ROS1* tyrosine kinases, through gene fusions, has been found in lung adenocarcinomas and are highly sensitive to selective kinase inhibitors. This study aimed at identifying the presence of these rearrangements in human colorectal adenocarcinoma (CRC) specimens using a 4-target, 4-color break-apart fluorescence in situ hybridization (FISH) assay to simultaneously determine the genomic status of *ALK* and *ROS1*. Among the clinical CRC specimens analyzed, rearrangement-positive cases for both *ALK* and *ROS1* were observed. The fusion partner for *ALK* was identified as EML4 and the fusion partner for one of the *ROS1*-positive cases was SLC34A2, the partner for the other *ROS1*-positive case remains to be identified. A small fraction of specimens presented duplicated or clustered copies of native *ALK* and *ROS1*. In addition, rearrangements were detected in samples that also harbored *KRAS* and *BRAF* mutations in two of the three cases. Interestingly, the *ALK*-positive specimen displayed marked intra-tumoral heterogeneity and rearrangement was also identified in regions of high-grade dysplasia. Despite the additional oncogenic events and tumor heterogeneity observed, elucidation of the first cases of *ROS1* rearrangements and confirmation of *ALK* rearrangements support further evaluation of these genomic fusions as potential therapeutic targets in CRC.

IMPLICATIONS

Implications: *ROS1* and *ALK* fusions occur in colorectal cancer and may have substantial impact in therapy selection.

Introduction

Activation of proto-oncogenes by genomic rearrangements resulting in the fusion of two unrelated genes was identified in leukemias and lymphomas decades ago and is an extensively explored mechanism of tumorigenesis as well as a basis for classification of hematopoietic neoplasms (1, 2). More recently, similar phenomena have been identified in a variety of solid tumors. Among these, rearrangement of the anaplastic lymphoma kinase (*ALK)* gene, originally identified in association with anaplastic large cell lymphoma (3), has been implicated in lung adenocarcinoma. Activation of *ALK* through gene fusions in lung cancer has been reported in approximately 5% of unselected lung adenocarcinomas, with increasing incidence when some clinicopathologic selection criteria are applied (4-17). The importance of this molecular diagnosis is that it predicts benefit from targeted kinase inhibitors. Patients with advanced *ALK*+ lung cancers, when treated with ALK inhibitors (e.g., crizotinib), have shown dramatic clinical response (18). The v-ros avian UR2 sarcoma virus oncogene homolog (*ROS1)* encodes a tyrosine kinase which shares significant homology with *ALK* and is activated by fusion events in 1.2-2.6% of lung cancer. Crizotinib is also clinically effective in lung cancer patients harboring these *ROS1* rearrangements (19-21). *ROS1* gene fusions have also been found in many other tumor types beyond lung cancer (22).

Colorectal cancer (CRC) is a major cause of cancer deaths worldwide. However, because existing therapies can be toxic, more specific therapeutic regimens such as targeted agents have been sought to improve the outcomes and quality of life of CRC patients. Efforts to identify alterations that could predict benefit from a targeted therapy approach in CRC have proven difficult. Whilst *KRAS* mutation analysis is an accepted molecular approach in CRC, unlike the demonstration of *EGFR* mutation or *ALK* rearrangement in NSCLC which are used to select patients for targeted therapies, *KRAS* mutational status is instead used to exclude patients unlikely to benefit from monoclonal anti-EGFR therapy.

Descriptions of fusion events such as *ALK* fusions in CRC have been rare as summarized in Table 1. In studies using reverse-transcriptase polymerase chain reaction (RT-PCR) for *EML4-ALK* fusions, no *ALK* rearrangements were found among 48 cases (8) and 96 cases (23) of CRC tested. *ALK* rearrangements were also not found by FISH in 12 colorectal neuroendocrine carcinoma cases (24), but *ALK* gene copy gain or amplification were found in 26 of 756 colorectal carcinoma cases(25). On the other hand, , *EML4-ALK* gene fusions were detected in 2 of 83 (2.4%) CRC specimens through exon array profiling (9), the *PRKAR1A-ALK* fusion was found in CRC by full exome sequencing(26), and the *C2orf44-ALK* fusion was found in 1 out of 40 (2.5%) CRC specimens tested by next generation sequencing (27). In this case, the in-frame fusion *C2orf44-ALK* resulted from a 5 megabase (MB) tandem duplication. The authors reported a ~90-fold increase in 3' *ALK* expression, suggesting that the *C2orf44-ALK* fusion transcript resulted in *ALK* kinase overexpression. Based on the presence of *ALK* rearrangements in CRC, and due to the extensive homology between *ALK* and *ROS1*, we hypothesized that *ROS1* genes may also be activated by gene fusions in CRC. Although there has been no report of *ROS1* activation in CRC to date, Lee et al (2013) recently reported 23 of 495 gastric adenocarcinoma cases (4.6%) with high level of *ROS1* expression by immunohistochemistry (28). Of these 23 cases, 3 were positive for gene rearrangement by FISH break-apart, two of which were found to present the *SLC34A2-ROS1* (S4:R32) fusion by RT-PCR (28). Additionally, in 2011, Gu et al reported 2 of 23 cases of cholangiocarcinoma that were positive for the GOPC (FIG)-ROS1 gene fusion using phosphotyrosine signaling profiling (mass spectrometry) followed by 5'RACE (29).

Overall, these findings suggest that an unrecognized subset of CRC may harbor genetic alterations predicting response to crizotinib and other targeted therapies. We herein analyzed the frequency of *ALK* and *ROS1* rearrangements in specimens from patients with metastatic CRC via FISH. In addition, we sought to identify the fusions partners in rearranged specimens through RT-PCR. Moreover, patients who harbored atypical *ALK* FISH patterns were further analyzed by RT-PCR to determine possible

rearrangements not detectable by FISH based on classically described definitions of FISH positivity (i.e. *C2orf44-ALK).*

Materials and Methods

Patients and Tissue Microarrays (TMA)

The tissue microarray was prepared using formalin fixed paraffin embedded (FFPE) CRC tissue specimens from 268 patients enrolled in the Australian Gastrointestinal Trials Group Randomized Phase III MAX Study(30), including all patients with adequate tissue available. These patients are representative (clinical, pathological characteristics) of the MAX phase III clinical trial population, as previously reported(31). All patients had histologically confirmed colorectal adenocarcinoma. Three tumor tissue cores per patient were distributed in 10 blocks, making up a 12x8 grid of cores on each slide. Thirty-nine of the patients were duplicated, and three were triplicated in the TMA for quality control. Institutional review board-approved informed consent was obtained by the MAX trial investigators for biomarker evaluation. Additional slides from the original pathology blocks of the positive samples were also made available for PCR and investigation of intra-tumoral heterogeneity.

FISH Assays and Analyses

The TMA slides were subjected to a *FISH* assay using a novel 4-color, 4-target *ALK*/*ROS1* break-apart probe (Abbott Molecular) developed to determine genomic status of *ALK* and *ROS1* in the same cells. *ALK* gene sequences were labeled in SpectrumRed (3'*ALK*) and SpectrumGreen (5'*ALK*); fused 5'/3' *ALK* signals were classified as normal, whereas split 5'-3' ALK by >2 diameters of the signal, and single 3'*ALK* were classified as abnormal (32). 3'*ALK* doublets-single green (RGR or RRG) was expected as the FISH pattern for the *C2orf44-ALK* fusion (27), thus this pattern was considered positive atypical. *ROS1* gene sequences were labeled in SpectrumAqua (3'*ROS1*) and SpectrumGold (5'*ROS1*); fused 5'-3'*ROS1*

signals were classified as normal, whereas split 5'-3'*ROS1* signals by >1 signal diameter, and single 5'*ROS1* or single 3'*ROS1* signals were classified as abnormal. For each patient, at least 50 tumor cells in two cores were scored. Variant patterns, such as the appearance of doublets or pairs, were annotated. A signal doublet was defined as the presence of two copies of the signal for a given target placed adjacently, that is, separated by ≤1 diameter of the average signal diameter; paired signals were defined as two fusion signals placed adjacently but separated by 1-2 diameters of the average signal. Doublet and paired signals were observed in hybridizations with both *ALK* and *ROS1* probes and, when present in >10% of cells, the specimen was classified as atypical. Some specimens displayed both fusion signal doublets and pairs, in which case they were included in the doublet category.

Using the same *ALK/ROS1* probe described above, additional FFPE slides of the resection blocks for the *ALK*+ patient were investigated for intra-tumoral heterogeneity. The FISH assays were performed using the Zymed Spot-Light Tissue Pretreatment kit (Invitrogen) in the TMAs and the Vysis Paraffin Pretreatment IV and Post-Hybridization Wash Buffer Kit (Abbott Molecular) in the sections, per manufacturers' instructions. Analysis was performed using interference filters sets for blue (DAPI), green (FITC), red (Texas Red), turquoise (Aqua) and yellow (Gold). Monochromatic images were acquired for each interference filter and merged using the CytoVision application (Leica Microsystems).

Reverse Transcriptase PCR

To identify the fusion partner for *ALK* and *ROS1*, reverse transcriptase (RT)-PCR was carried out as described using the SuperScript III First-Strand Synthesis System (Invitrogen) with previously published *ALK* and *ROS1* primers; the *ALK* primer was located in exon 20 (*ALK* Rev20; (13)), whereas the *ROS1* primer was located in exon 34 (*ROS1* E34R; (33)). First-strand synthesis was carried out as above followed by a 20-minute RNaseH digestion at 37°C. Individual PCR reactions were carried out to amplify either *EML4-ALK* or *C2orf44-ALK*, using previously published primers for exon 6, exon 13 and exon 18 of

EML4 and exon 20 of *ALK* (*ALK* Sanders R20 (13) and an in-house primer for *C2orf44 (*C2orf44fwd1)). Likewise, individual PCR reactions were carried out to amplify either *SLC34A2-ROS1*, *CD74-ROS1*, or *SDC4-ROS1* using the previously published primers (*SLC34A2:E4F*, *CD74:E5F*, *ROS1*:E34F (20)) along with a primer to *SDC4* of our design (*SDC4-E2F*; (33)). PCR conditions for detecting the *ALK* and *ROS1* fusion partners included an initial denaturation at 95°C for 5 min followed by 10 cycles of touchdown PCR and 30 cycles of PCR. PCR products were resolved on a 2% agarose gel. Positive PCR products were excised from agarose gel, purified (Wizard SV Gel and PCR Clean Up Kit; Promega), and sequenced. All primer sequences are listed in Supplementary Table 1.

Microdissection and Mutation Analysis

KRAS and BRAF mutational analysis was performed initially on CRC specimens used in the TMA using high-resolution melting point (HRM) PCR as previously reported (34). Subsequently for specimens where *ALK* or *ROS1* rearrangements were identified with *KRAS* or *BRAF* mutations, tumor areas were identified and areas for differential microdissection were mapped based on parallel Hematoxylin and Eosin stained slide. 4µm sections were deparaffinized, hematoxylin counterstained and microdissected by scalpel point under microdissecting microscope. Microdissected material was washed with 70% ethanol, air dried, and resuspended in lysis buffer and DNA extracted (Qiagen QIAamp DSP DNA FFPE Tissue Kit (#60404) using manual extraction with elution into 30 microliters of elution buffer.

For first round mutational analysis, DNA samples from selectively microdissected areas were PCR amplified with primers flanking *KRAS* exon 2 as previously described (35), followed by Sanger DNA sequencing. Positive samples for mutation by Sanger sequencing were not further evaluated, negative samples were evaluated by HRM curve to achieve higher analytical sensitivity. Briefly, DNA samples from selectively microdissected areas were PCR amplified with primers flanking *KRAS* exon 2 on the Roche LightCycler 480 using the Roche LC480 High Resolution Melting Master Kit (#04909631001).

Resulting real-time PCR curves were evaluated for perturbations in the melting curve profiles with appropriate controls. The HRM assay was estimated to have an analytical sensitivity of ~5% based on dilution studies.

Results

Demonstration of ALK and ROS1 Fusions in CRC

Of the 268 patient specimens originally included in the tissue microarray, 236 had evaluable FISH results defined as at least 50 tumor cells in two cores. The cutoff threshold for positivity was identified as ≥15% of cells displaying patterns compatible with rearrangement, based on the distribution of relevant patterns in the cohort with application of evaluation of mean + 3x standard deviation of signal and beta inverse function (data not shown). Two cases (0.8%) demonstrated FISH patterns consistent with *ROS1* rearrangement, predominantly single 3'*ROS1* signals (Figures 1A, B). One case (0.4%) demonstrated a pattern consistent with *ALK* rearrangement, and it also had predominantly single 3'*ALK* signals (Figure 1C). The atypical pattern 3' *ALK* doublets (3'/5'/3'*ALK*) associated with the *C2orf44-ALK* fusion were identified in 7 cases (3%), subjected later to RT-PCR testing. Other signal variants were identified for both *ALK* and *ROS1*, including 25 cases with 3'/5' fusion *ALK* doublets (10.6%), and 12 cases each (5.1%) with 3'*ROS1* doublets (3'/5'/3'*ROS1*) and 3'/5' fusion doublets for *ROS1*.

In patient #406 (*ALK* positive), the primary tumor site was the rectum with metastases of lymph nodes and lung. In patient #38 (*ROS1* positive), the primary tumor site was the ascending colon with metastases in lymph nodes and liver. In patient #100 (*ROS1* positive) the primary tumor site was the rectum and the sigmoid colon with metastasis in the lung. These patients were, respectively, 84 (female), 78 (male) and 69 (female) years old at the time at which their metastatic disease was diagnosed..

Original pathology blocks from the identified cases were evaluated by RT-PCR to further verify the presence of fusion events. RT-PCR spanning previously published *ROS1* breakpoints paired with specific primers for known fusion partners of *ROS1* was employed. Of the two cases demonstrating FISH patterns consistent with *ROS1* fusion events, one was confirmed by RT-PCR to harbor a *SLC34A2-ROS1* fusion (exons 4 and 34, respectively; Figure 1D) while the second case was negative for all known fusion partners of *ROS1*. Similarly, RT-PCR assays spanning previously published *ALK* breakpoints paired with specific primers for known fusion partners of *ALK* were employed. The case identified as consistent with *ALK* rearrangement demonstrated the presence of an *EML4-ALK* rearrangement (exons 6 and 20, respectively; Figure 1E). The seven cases identified as atypical with 3'*ALK* doublets (3'/5'/3' *ALK* fusion) were all negative for known fusion partners of *ALK*, including *C2orf44*. Specimens with other variants were also tested, when available, by RT-PCR and no fusion was detected.

Of note, the specimen with *SLC34A2-ROS1* fusion and the *ALK*+ case were previously classified as positive for *BRAF [c.1799T>A (p.V600E)]* and *KRAS [c.35G>C (p.G12A)]* mutations, respectively, during routine clinical testing.

Identification of Intra-Tumoral Heterogeneity

In the case identified with *ALK* rearrangement, three tissue cores containing tumor were subjected to analysis, however only two of the three cores demonstrated the finding of *ALK* rearrangement by FISH. Pathologic evaluation confirmed the presence of tumor in the core negative for *ALK* rearrangement, and confirmed morphology of the tumor compatible with the other two tissue cores. This finding was suggestive of intratumoral heterogeneity, which was further explored by evaluation of two tissue blocks from the source material. Multiple tissue areas from each of two tumor blocks were selected for additional FISH evaluation. Areas were marked on a parallel H&E stained section, and each region was separately evaluated for the presence of *ALK* rearrangement by FISH.

Analysis of one block demonstrated a marked separation between areas of tumor that were positive and negative for *ALK* rearrangement by FISH (Figure 2A). Analysis of the second block demonstrated multiple areas of tumor with positive and negative patterns for *ALK* rearrangement in a more interposed distribution (Figure 2B). Histologic evaluation demonstrated that some of the tissue areas identified as positive for *ALK* rearrangement were pathologically best classified as high-grade dysplasia (Figures 2C, D).

Given that the specimen with heterogeneity for *ALK* rearrangement was classified as *KRAS* positive during routine clinical analysis, we sought to determine whether the *ALK* status overlapped with *KRAS* status within sub-regions of the tumor. Areas of tumor which were parallel to those evaluated by FISH were separately microdissected and *KRAS* mutation status ascertained by Sanger sequencing and, when negative, also by high-resolution melting curve analysis. These analyses demonstrated that some areas of the tumor retained positivity for *KRAS* mutation (Figure 3A) while other regions showed all four possible combinations of *ALK*/*KRAS* status (Figure 3B).

The finding of intratumoral heterogeneity with respect to both *ALK* and *KRAS* alterations also led to the question of whether such heterogeneity was observed in either case with *ROS1* rearrangement. However, no evidence of intratumoral heterogeneity with respect to *ROS1* rearrangement was identified, therefore further analysis of intratumoral heterogeneity *BRAF* mutation in the *ROS1*+ case was not pursued.

Discussion

Previous reports of gene fusions involving *ALK* in CRC indicate that these events are rare, and our findings are consistent with reported studies demonstrating a low but detectable rate of *ALK* rearrangement in CRC. In addition, this study is the first to demonstrate a similarly low but detectable rate of *ROS1* rearrangement in CRC. The demonstration of a fusion product by RT-PCR in two of the

three rearrangement-positive cases confirms the FISH findings and serves to underscore the importance of further characterization of these fusion events in CRC. The absence of a detectable fusion product in the third case (*ROS1* positive) is likely attributable to an unknown fusion partner. These findings have potentially significant therapeutic implications, as identification of these rearrangements may open the possibility for targeted therapy.

Of particular note, 2 of the 3 cases positive for fusion events were found in concert with oncogene point mutation events (*KRAS* and *BRAF*). This is in contrast to the predominant findings in NSCLC, which show that concurrent 'driver' mutations such as *EGFR* mutation and *ALK* rearrangements may occur but are uncommon (36-39). This result is of particular clinical relevance as attempts to identify CRC cases harboring these fusion events cannot benefit from an enrichment strategy where patients with KRAS or BRAF mutations are excluded from further testing.

A surprising result in this study was the demonstration of marked intratumoral heterogeneity for both *KRAS* mutation and *ALK* rearrangement status. Moreover, the identification of all four combinations of *KRAS* and *ALK* status throughout the specimen was particularly unexpected, as was the identification of a region of high-grade dysplasia harboring both molecular alterations. Multiple studies have indicated that not only is *KRAS* mutation an early event in colorectal carcinoma tumorigenesis, but it shows a very low discordance rate between primary tumor and corresponding metastasis (40, 41). These findings often support the notion that *KRAS* mutation is both homogeneously distributed and required for tumor perpetuation. However, recent studies have demonstrated that marked intratumoral heterogeneity does exist (42). Importantly, the current study was performed retrospectively, and none of the three patients identified with fusion events were treated with targeted therapy agents specific to those fusion products prior to death.

High-grade dysplasia is the precursor lesion to invasive carcinoma in the lower gastrointestinal tract, and the identification of a region of high-grade dysplasia harboring both *KRAS* mutation and *ALK* rearrangement is intriguing and creates the basis for several hypotheses explaining mechanisms by which all four combinations of *KRAS* and *ALK* status might exist through clonal evolution (Figure 3). In each of these hypotheses, the originating cell is negative for both alterations, and a gain of one alteration is the first step. One possibility is that the gain of alteration is step-wise (Figures 4A, B), in which either *KRAS* or *ALK* is sequentially gained in the neoplastic population. In order for this 'sequential gain' hypothesis to then yield a fourth species, the population must, by definition, undergo a 'loss event'. Alternatively, the gains of alterations could first be in parallel, in which separate populations of cells independently gain either *KRAS* mutation or *ALK* rearrangement (Figure 4C). This 'separate gain' hypothesis would then require that a second event occur in order to generate a fourth species. Lastly, the possibility that the technology used to interrogate *KRAS* mutation status and *ALK* rearrangement is not sufficiently sensitive to determine whether the alterations actually occur in the same cells is a consideration, and gives rise to a 'separate clones' hypothesis (Figure 4D). Among these possibilities, we regard the separate gain hypothesis and the sequential gain hypothesis with *ALK* rearrangement occurring prior to *KRAS* mutation to be the least likely of these events, largely because of the substantial volume of data demonstrating *KRAS* mutation commonly occurring in adenomatous lesions.

These potential hypotheses regarding the genesis of the observed spectrum of sub-species in this heterogeneous lesion have several putative functional considerations. One possibility is that *KRAS* mutation is a 'driver' and *ALK* rearrangement observed functionally acts as a 'passenger'. This explanation does not sufficiently explain the finding of *ALK*+/*KRAS*- regions. Similarly, the *ALK* rearrangement may be a modulator of tumor growth, which is also difficult to reconcile with the finding of *ALK*+/*KRAS*- regions. Another possibility, best hypothesized in the 'separate clones' explanation is that *KRAS* and *ALK* represent dual drivers with subclonal evolution. This hypothesis is best considered in the

context of underlying genomic instability, which could fuel random events expressed as subclonal heterogeneity.

The findings of this study have several specific implications with regard to future analysis of colorectal carcinoma. These data strongly support further evaluation of colorectal carcinoma for fusion events in *ALK* and *ROS1*, and further suggest the possibility that these events may serve as targets for therapy in CRC. As mentioned, the overlap of these fusions with both *KRAS* and *BRAF* mutations is a potential confounding factor, as not only does it impact approaches to screening, but these alterations may also modulate responsiveness to targeted therapy agents. Based on our findings, it may be challenging to identify a substantial number of patients with a uniform molecular profile with regard to fusion events and mutation status. The screening process itself may be impacted by these findings, which suggest that multiple regions of tumor may need to be evaluated. Furthermore, these findings highlight the technological hurdles involved in evaluation of tumor heterogeneity, and underscore the importance of methodologies to evaluate mutation status on a single-cell *in situ* basis.

Acknowledgment: Study was partially supported by research grants from Abbott Molecular to MVG, Boettcher Foundation to RCD, and the NCI CCSG P30CA046934 (Molecular Pathology Shared Resource). TN was supported by the Cancer Research Summer program from the University of Colorado Cancer Center; DDP was a fellow from the Brazilian Agency CAPES; AJW was supported by an NHRMC post graduate Fellowship and Roche HOTT Fellowship. Authors thank Lisa Litzenberger for graphics assistance.

References

1. WHO Classification of Tumours of Haematopoietic and Lymphoid Tissues. 4th ed. Lyon: International Agency for Research on Cancer; 2008.
2. Mitelman F, Johansson B, Mertens F. The impact of translocations and gene fusions on cancer causation. Nat Rev Cancer 2007;7:233-45.
3. Morris SW, Kirstein MN, Valentine MB, Dittmer KG, Shapiro DN, Saltman DL, et al. Fusion of a kinase gene, ALK, to a nucleolar protein gene, NPM, in non-Hodgkin's lymphoma. Science 1994;263:1281-4.
4. Rikova K, Guo A, Zeng Q, Possemato A, Yu J, Haack H, et al. Global survey of phosphotyrosine signaling identifies oncogenic kinases in lung cancer. Cell 2007;131:1190-203.
5. Soda M, Choi YL, Enomoto M, Takada S, Yamashita Y, Ishikawa S, et al. Identification of the transforming EML4-ALK fusion gene in non-small-cell lung cancer. Nature 2007;448:561-6.
6. Choi YL, Takeuchi K, Soda M, Inamura K, Togashi Y, Hatano S, et al. Identification of novel isoforms of the EML4-ALK transforming gene in non-small cell lung cancer. Cancer Res 2008;68:4971-6.
7. Koivunen JP, Mermel C, Zejnullahu K, Murphy C, Lifshits E, Holmes AJ, et al. EML4-ALK fusion gene and efficacy of an ALK kinase inhibitor in lung cancer. Clin Cancer Res 2008;14:4275-83.
8. Takeuchi K, Choi YL, Soda M, Inamura K, Togashi Y, Hatano S, et al. Multiplex reverse transcription-PCR screening for EML4-ALK fusion transcripts. Clin Cancer Res 2008;14:6618-24.
9. Lin E, Li L, Guan Y, Soriano R, Rivers CS, Mohan S, et al. Exon array profiling detects EML4-ALK fusion in breast, colorectal, and non-small cell lung cancers. Mol Cancer Res 2009;7:1466-76.
10. Takeuchi K, Choi YL, Togashi Y, Soda M, Hatano S, Inamura K, et al. KIF5B-ALK, a novel fusion oncokinase identified by an immunohistochemistry-based diagnostic system for ALK-positive lung cancer. Clin Cancer Res 2009;15:3143-9.
11. Wong DW, Leung EL, So KK, Tam IY, Sihoe AD, Cheng LC, et al. The EML4-ALK fusion gene is involved in various histologic types of lung cancers from nonsmokers with wild-type EGFR and KRAS. Cancer 2009;115:1723-33.
12. Takahashi T, Sonobe M, Kobayashi M, Yoshizawa A, Menju T, Nakayama E, et al. Clinicopathologic features of non-small-cell lung cancer with EML4-ALK fusion gene. Ann Surg Oncol 2010;17:889-97.
13. Sanders HR, Li HR, Bruey JM, Scheerle JA, Meloni-Ehrig AM, Kelly JC, et al. Exon scanning by reverse transcriptase-polymerase chain reaction for detection of known and novel EML4-ALK fusion variants in non-small cell lung cancer. Cancer Genet 2011;204:45-52.
14. Wong DW, Leung EL, Wong SK, Tin VP, Sihoe AD, Cheng LC, et al. A novel KIF5B-ALK variant in nonsmall cell lung cancer. Cancer 2011;117:2709-18.
15. Jung Y, Kim P, Jung Y, Keum J, Kim SN, Choi YS, et al. Discovery of ALK-PTPN3 gene fusion from human non-small cell lung carcinoma cell line using next generation RNA sequencing. Genes Chromosomes Cancer 2012;51:590-7.
16. Soda M, Isobe K, Inoue A, Maemondo M, Oizumi S, Fujita Y, et al. A prospective PCR-based screening for the EML4-ALK oncogene in non-small cell lung cancer. Clin Cancer Res 2012;18:5682-9.
17. Togashi Y, Soda M, Sakata S, Sugawara E, Hatano S, Asaka R, et al. KLC1-ALK: a novel fusion in lung cancer identified using a formalin-fixed paraffin-embedded tissue only. PLoS One 2012;7:e31323.
18. Camidge DR, Bang YJ, Kwak EL, Iafrate AJ, Varella-Garcia M, Fox SB, et al. Activity and safety of crizotinib in patients with ALK-positive non-small-cell lung cancer: updated results from a phase 1 study. Lancet Oncol 2012;13:1011-9.
19. Bergethon K, Shaw AT, Ou SH, Katayama R, Lovly CM, McDonald NT, et al. ROS1 rearrangements define a unique molecular class of lung cancers. J Clin Oncol 2012;30:863-70.

20. Davies KD, Le AT, Theodoro MF, Skokan MC, Aisner DL, Berge EM, et al. Identifying and targeting ROS1 gene fusions in non-small cell lung cancer. Clin Cancer Res 2012;18:4570-9.
21. Ou S, Bang Y, Camidge D, Riely G, Salgia R, Shapiro G, et al. Efficacy and safety of crizotinib in patients with advanced ROS1-rearranged non-small cell lung cancer (NSCLC). ASCO Meeting Abstracts 2013;31:8032.
22. Davies KD, Doebele RC. Molecular Pathways: ROS1 Fusion Proteins in Cancer. Clin Cancer Res 2013.
23. Fukuyoshi Y, Inoue H, Kita Y, Utsunomiya T, Ishida T, Mori M. EML4-ALK fusion transcript is not found in gastrointestinal and breast cancers. Br J Cancer 2008;98:1536-9.
24. Karkouche R, Bachet JB, Sandrini J, Mitry E, Penna C, Cote JF, et al. Colorectal neuroendocrine carcinomas and adenocarcinomas share oncogenic pathways. A clinico-pathologic study of 12 cases. Eur J Gastroenterol Hepatol 2012;24:1430-7.
25. Bavi P, Jehan Z, Bu R, Prabhakaran S, Al-Sanea N, Al-Dayel F, et al. ALK gene amplification is associated with poor prognosis in colorectal carcinoma. Br J Cancer 2013.
26. Eddy S, Tomilo M, Urick ME, Khazanov MA, Williams P, Bankhead A, et al. Expanded clinical opportunities for crixotinib from analysis of over 5,000 cancer patient exomes. AACR-NCI-EORTC International Conference on Molecular Targets and Cancer Therapeutics 2013:abstract C256.
27. Lipson D, Capelletti M, Yelensky R, Otto G, Parker A, Jarosz M, et al. Identification of new ALK and RET gene fusions from colorectal and lung cancer biopsies. Nat Med 2012;18:382-4.
28. Lee J, Lee SE, Kang SY, Do IG, Lee S, Ha SY, et al. Identification of ROS1 rearrangement in gastric adenocarcinoma. Cancer 2013;119:1627-35.
29. Gu TL, Deng X, Huang F, Tucker M, Crosby K, Rimkunas V, et al. Survey of tyrosine kinase signaling reveals ROS kinase fusions in human cholangiocarcinoma. PLoS One 2011;6:e15640.
30. Tebbutt NC, Wilson K, Gebski VJ, Cummins MM, Zannino D, van Hazel GA, et al. Capecitabine, bevacizumab, and mitomycin in first-line treatment of metastatic colorectal cancer: results of the Australasian Gastrointestinal Trials Group Randomized Phase III MAX Study. J Clin Oncol 2010;28:3191-8.
31. Weickhardt AJ, Williams D, Lee C, Simes J, Murone C, Wilson K, et al. Vascular endothelial growth factors (VEGF) and VEGF receptor expression as predictive biomarkers for benefit with bevacizumab in metastatic colorectal cancer (mCRC): Analysis of the phase III MAX study. ASCO Meeting Abstracts 2011;29:3531.
32. Camidge DR, Kono SA, Flacco A, Tan AC, Doebele RC, Zhou Q, et al. Optimizing the detection of lung cancer patients harboring anaplastic lymphoma kinase (ALK) gene rearrangements potentially suitable for ALK inhibitor treatment. Clin Cancer Res 2010;16:5581-90.
33. Li C, Fang R, Sun Y, Han X, Li F, Gao B, et al. Spectrum of oncogenic driver mutations in lung adenocarcinomas from East Asian never smokers. PLoS One 2011;6:e28204.
34. Price TJ, Hardingham JE, Lee CK, Weickhardt A, Townsend AR, Wrin JW, et al. Impact of KRAS and BRAF Gene Mutation Status on Outcomes From the Phase III AGITG MAX Trial of Capecitabine Alone or in Combination With Bevacizumab and Mitomycin in Advanced Colorectal Cancer. Journal of clinical oncology : official journal of the American Society of Clinical Oncology 2011;29:2675-82.
35. Franklin WA, Haney J, Sugita M, Bemis L, Jimeno A, Messersmith WA. KRAS mutation: comparison of testing methods and tissue sampling techniques in colon cancer. J Mol Diagn 2010;12:43-50.
36. Alrifai D, Popat S, Ahmed M, Gonzalez D, Nicholson AG, Parcq J, et al. A rare case of squamous cell carcinoma of the lung harbouring ALK and BRAF activating mutations. Lung Cancer 2013;80:339-40.
37. An SJ, Chen ZH, Su J, Zhang XC, Zhong WZ, Yang JJ, et al. Identification of enriched driver gene alterations in subgroups of non-small cell lung cancer patients based on histology and smoking status. PLoS One 2012;7:e40109.

38. Boland JM, Jang JS, Li J, Lee AM, Wampfler JA, Erickson-Johnson MR, et al. MET and EGFR mutations identified in ALK-rearranged pulmonary adenocarcinoma: molecular analysis of 25 ALK-positive cases. J Thorac Oncol 2013;8:574-81.
39. Zhang X, Zhang S, Yang X, Yang J, Zhou Q, Yin L, et al. Fusion of EML4 and ALK is associated with development of lung adenocarcinomas lacking EGFR and KRAS mutations and is correlated with ALK expression. Mol Cancer 2010;9:188.
40. Watanabe T KT, Yamamoto Y, Matsuda K, Ishihara S, Nozawa K, Iinuma H, Shibuya H, Eshima K. Heterogeneity of KRAS status may explain the subset of discordant KRAS status between primary and metastatic colorectal cancer. Dis Colon Rectum 2011;54:1170-8.
41. Mariani P, Lae M, Degeorges A, Cacheux W, Lappartient E, Margogne A, et al. Concordant analysis of KRAS status in primary colon carcinoma and matched metastasis. Anticancer Res 2010;30:4229-35.
42. Gerlinger M, Rowan AJ, Horswell S, Larkin J, Endesfelder D, Gronroos E, et al. Intratumor heterogeneity and branched evolution revealed by multiregion sequencing. N Engl J Med 2012;366:883-92.

Table 1.

Gene	Reference	Tumor Type	Technology	# Tested	# Positive	Fusion Partner*
ALK	Fukuyoshi et al.(23)	Colorectal Carcinoma	RT-PCR for *EML4*	96	0	NA
	Takeuchi et al.(8)	Colon Carcinoma	RT-PCR for *EML4*	48	0	NA
	Lin et al.(9)	Colorectal Carcinoma	Exon-Array Profiling and RT-PCR for *EML4*	83	2	*EML4* E20 and E21
	Karkouche et al.(24)	Colorectal Neuroendocrine Carcinoma	FISH	12	0	NA
	Lipson et al.(27)	Colorectal Carcinoma	Next Generation Sequencing	40	1	*C2orf44*
	Bavi et al.(25)	Colorectal Carcinoma	FISH	756	0	NA
	Eddy et al.(26)	Full Exome Sequencing	Full Exome Sequencing	NA*	NA*	*PRKAR1A , EML4*
ROS1	Lee et al.(28)	Gastric Adenocarcinoma	FISH then RT-PCR for identification of fusion partner	495	3	*SLC34A2* (x2); 1 unknown
	Gu et al.(29)	Cholangiocarcinoma	Phosphotyrosine signaling profiling (mass spectrometry) followed by 5'RACE	23	2	*GOPC (FIG)* E3 and E7

- NA: Not Applicable; NA*: Data not available E: exon of the partner gene fused to *ALK* or *ROS1*

Table and Figure Legends

Table 1: Summary of published reports evaluating *ALK* and *ROS1* rearrangements in tumors of the gastrointestinal system

Figure 1: A, B) FISH images showing *ROS1* rearrangement in two specimens as demonstrated by single 3' *ROS1* (aqua) signals; C) FISH image demonstrating *ALK* rearrangement based on single 3'*ALK* (red) signals; D) Sequencing of RT-PCR product from the sample depicted in panel A confirming *ROS1* fusion with *SLC34A2*; E) Sequencing of RT-PCR product from the sample depicted in panel C confirming *EML4-ALK* fusion.

Figure 2: A, B) Two blocks from the original specimen utilized for TMA demonstrated areas with varying patterns of *ALK* rearrangement and *KRAS* mutation status. Red circled areas indicate *ALK* rearranged and mutated *KRAS* (*ALK*+/*KRAS*+). Blue circled areas indicate *ALK* wild-type and *KRAS* mutated (*ALK*-/*KRAS*+). Green circled areas indicated *ALK* rearranged and *KRAS* wild-type (*ALK*+/*KRAS*-). Black areas indicate wild-type for both alterations (*ALK*-/*KRAS*-). C, D) Higher magnification of the regions indicated in panel E by yellow arrows demonstrates that some regions are best classified as high-grade dysplasia. FISH analysis in region F was positive for *ALK* rearrangement and FISH analysis in region G was negative for *ALK* rearrangement (FISH images not shown).

Figure 3: A) Representative sequencing findings of *KRAS* mutated area. B) Representative high-resolution melting analysis of regions negative for *KRAS* mutation by sequencing. Blue curves show overlap of tested regions with wild-type control, red and green show positive controls (2 distinct mutations)

Figure 4: Possible mechanisms to explain findings of different combinations of *ALK* rearrangement and *KRAS* mutation status.

Figure 1

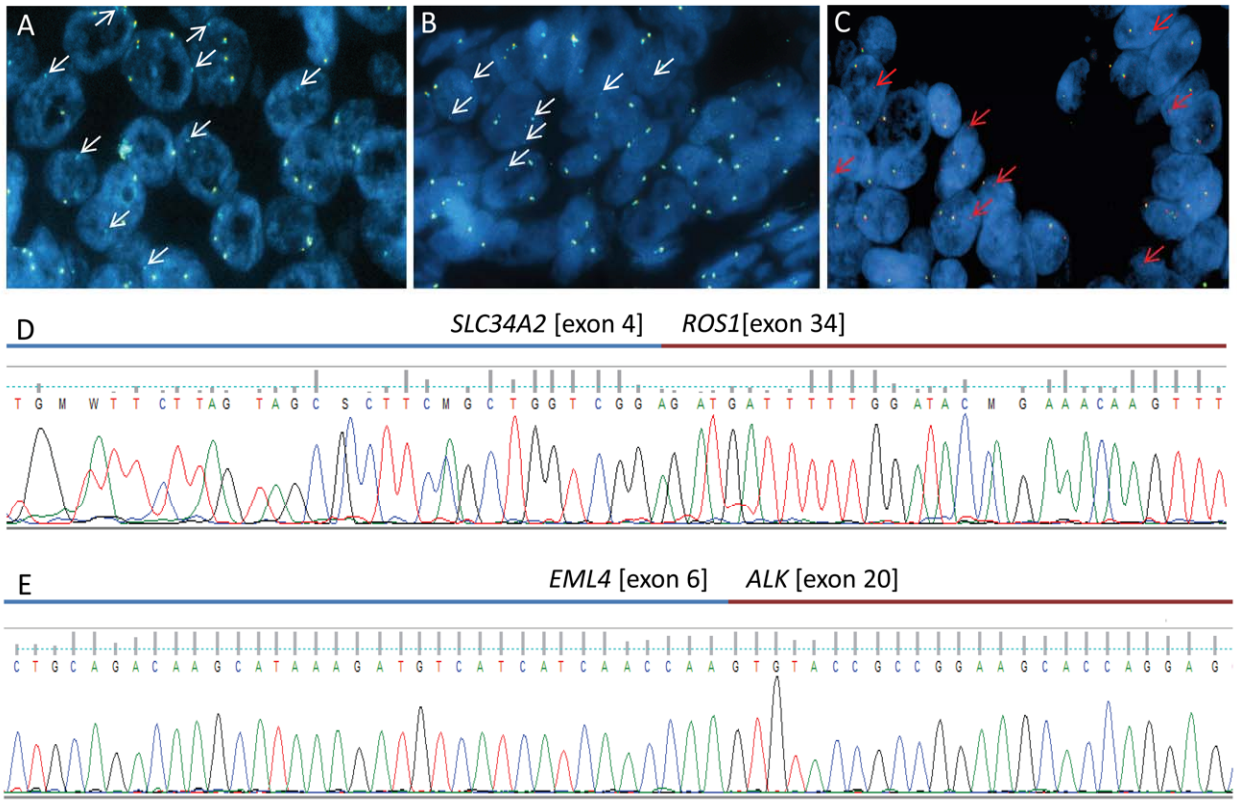

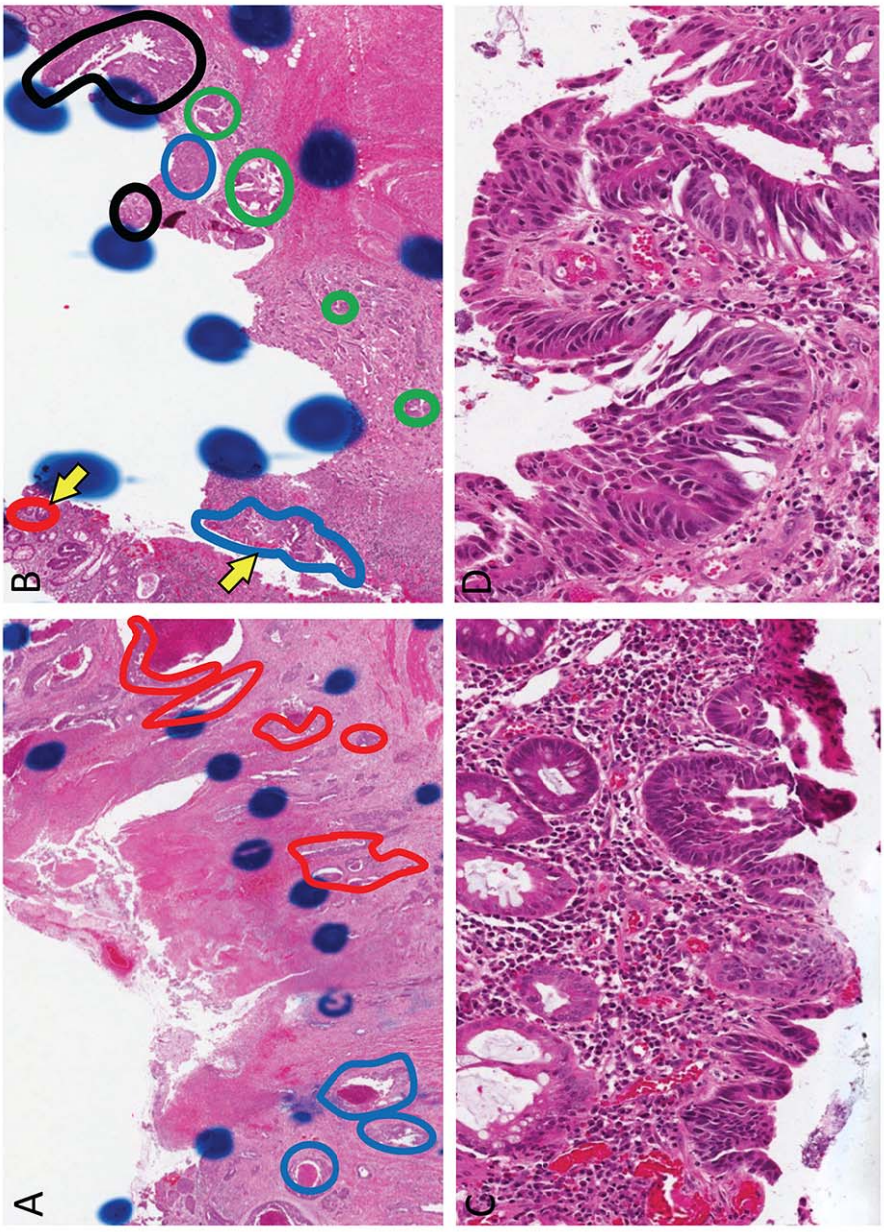

Figure 2

Figure 3

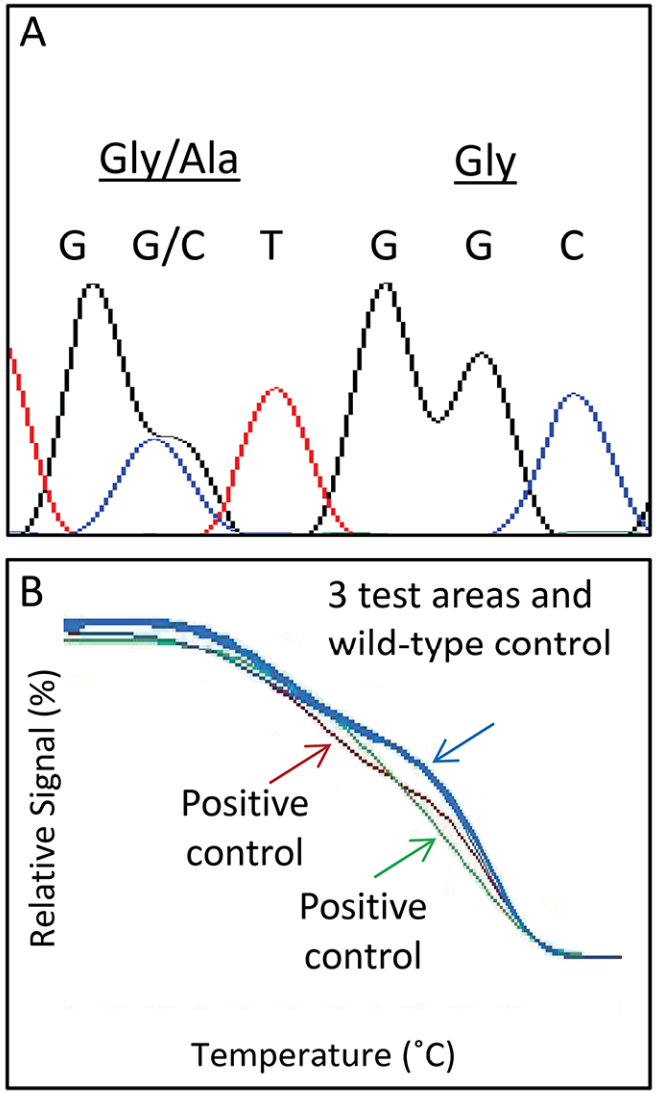

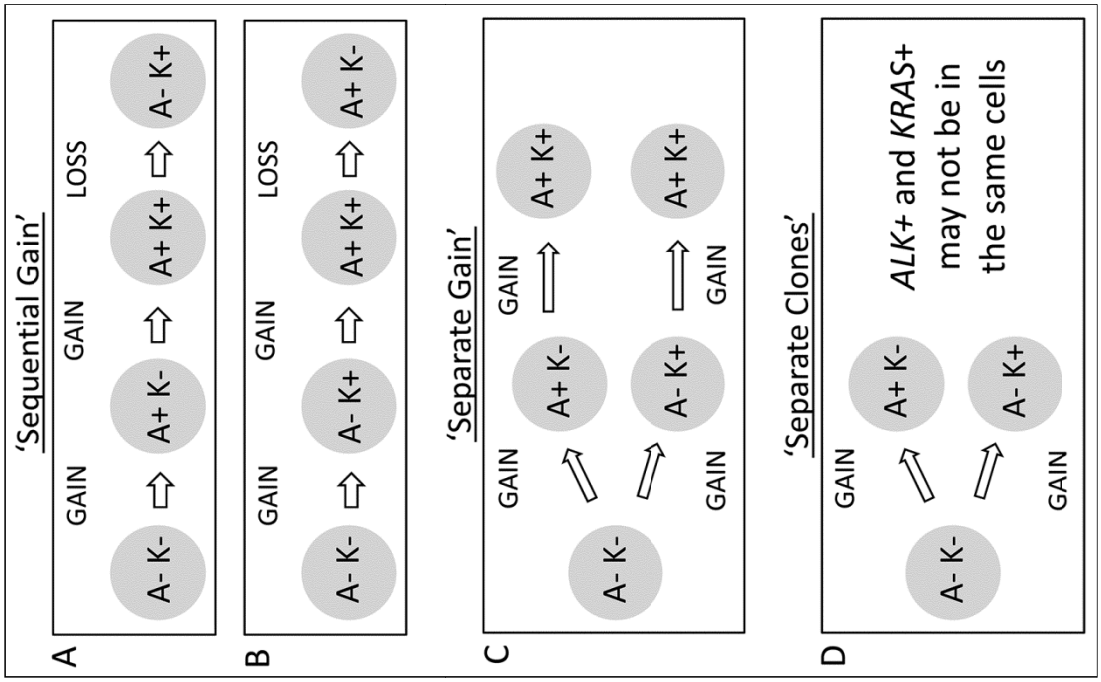

Figure 4